Polarization switching of ring microstrip antennas fed by an L-probe with PIN diodes

Kenta Yamaura, # Yuichi Kimura, and Misao Haneishi

Department of Electrical and Electronic Systems, Saitama University
255 Shimo-ohkubo, Sakura-ku, Saitama 338-8570, Japan
ykimura@aplab.ees.saitama-u.ac.jp

1. Introduction

Microstrip antennas (MSAs) are widely used for various purposes such as mobile communications and satellite communications due to its low profile, lightweight, and simple configuration [1]-[2]. The authors have developed a multi-ring MSA for multi-band operation [3]-[4]. This antenna consists of multiple square ring patches corresponding to number of operation frequencies and an L-probe for feeding them. Each ring patch radiates either linear polarization or circular polarization by tuning truncated corners of the patch. On the other hand, polarization control of microstrip antennas with PIN diodes is reported by many papers [5]-[8].

In order to realize a multi-band planar antenna for switchable polarization, this paper presents performance of polarization switching of ring MSAs with PIN diodes. By changing ON and OFF of two PIN diodes on adjacent corners of a square ring patch, orthogonal currents are excited on the ring patch. Thus, orthogonal linear polarizations can be switched by bias currents of the PIN diodes. Two types of bias circuits for PIN diodes, on the same layer as the ring patch and on the backside of the ground plane, are discussed for one ring MSA. Then, the latter type of the bias circuit is applied to two ring MSAs for dual band operation.

2. A ring MSA with a bias circuit on the same layer

Figure 1 presents a configuration of a ring MSA for switchable polarization. The whole structure consists of two dielectric substrate with relative dielectric constant ε_r of 2.6, loss tangent $\tan\delta$ of 1.8×10^{-4}, and thickness of 1.2 mm. A square ring patch is on the top surface of the upper substrate and a coaxial cable is connected to an L-probe formed in the bottom substrate to realize good impedance matching to the ring MSA. Two PIN diodes P_1 and P_2 are situated on adjacent corners of the ring patch. DC bias circuits are arranged on the same layer as the ring patch and are connected to the ring patch at the centres of the top and bottom edges, respectively. The bias circuits perform as RF chokes. When the upper bias circuit is set to higher voltage than the lower one, P_2 turns ON and P_1 turns OFF. Then, the current on the ring patch flows from the lower-left corner to the upper-right one. Thus, a tilted polarization of $\phi = +45$ deg. is observed at the broadside. On the contrary, when the lower bias circuit is set to higher voltage, P_1 turns ON and P_2 turns OFF, then a tilted polarization of $\phi = -45$ deg. is observed at the broadside. In this design, the bias circuits are bent to be symmetrical with respect to the horizontal axis in order to cancel out undesirable radiation from the bias circuits at the broadside.

A prototype antenna as shown in Fig. 1 is manufactured. Figure 2 compares simulated and measured return loss characteristics of the prototype, where the simulated results are obtained by using Zealand IE3D. Minimum return loss is observed at slightly higher frequencies than the simulated one for both cases of P_1 ON and P_2 ON, respectively, because accurate equivalent circuit of the PIN diode is not taken into account in the simulation. Figure 3 compares simulated and measured polarization characteristics, where angle ϕ indicates a polarization angle corresponding to a direction of E-field vector observed at the broadside. From this figure, it is confirmed that linear polarizations of $\phi = \pm 45$ deg. are realized. Figure 4 (a) to (d) present radiation patterns in the E- and H-planes for P_1 ON and P_2 ON, respectively. Good unidirectional patterns are obtained and the

simulated and the measured patterns are in good agreement for co-polarizations, while slightly large cross polarizations are observed.

3. A ring MSA with a bias circuit on the backside

Figure 5 presents a configuration of a ring MSA with two PIN diodes, for which bias circuits are arranged on the backside of the ground plane in order to reduce the undesirable radiation from the bias circuits. One more dielectric substrate with the same dielectric constant and loss tangent, and thickness of 0.6 mm is added on the backside and the bottom bias circuits and the top ring patch are connected through vias. Furthermore, the bias circuits are miniaturized for dual band operation in the following. Figure 6 shows simulated and measured return loss characteristics of the prototype antenna as shown in Fig. 5. Similarly, the frequencies where minimum return loss is measured are slightly higher than the simulated ones for both P_1 ON and P_2 ON, respectively. Figure 7 presents the polarization characteristics and reveals that linear polarizations of $\phi = \pm 45$ deg. are observed. Figure 8 (a) to (d) present radiation patterns in the E- and H-planes for P_1 ON and P_2 ON, respectively. The cross polarizations are reduced in comparison with Fig. 4,

4. Two ring MSAs for dual band operation

Figure 9 presents a configuration of two ring MSAs for dual band operation, where two PIN diodes are mounted on each ring patch. Bias circuits are arranged on the backside of the ground plane for each ring patch. Figure 10 shows return loss characteristics of a prototype as shown in Fig. 9. Minimum return losses are observed at around 2.75 GHz for 1st mode and 4.73 GHz for 2nd mode. Figure 11 shows the polarization characteristics. $\phi = \pm 45$ deg. polarizations are obtained for 1st mode. However, $\phi = -45$ deg. and +20 deg. polarizations are observed for 2nd mode, which should be improved in the future. Figure 11 (a) to (d) present radiation patterns in the E- and H-planes of 1st mode and 2nd mode for P_1 ON, respectively. Good unidirectional patterns are obtained for co-polarizations and low cross polarizations below –20 dB are measured at the broadside.

5. Conclusions

This paper discusses performance of switchable polarization of ring MSAs with PIN diodes. In order to reduce the undesired radiation, the bias circuits are arranged on the backside of the ground plane and then $\phi = \pm 45$ deg. polarizations as well as reduction of the cross polarization levels are confirmed. Furthermore, PIN diodes and the bias circuits mentioned above are applied to two ring MSAs for dual band operation. Improvement of polarization characteristics of 2nd mode is left for future study.

References

[1] M. Haneishi, K. Hirasawa, and Y. Suzuki, *Small and planar antennas*, IEICE, 1996.

[2] M. Haneishi, "Technical features, applied technology, and perspectives of planar antennas," *IEICE Trans. Electron.*, vol. J89-C, no. 5, pp. 198-209, May 2006.

[3] Y. Shinohe, M. Haneishi, and Y. Kimura, "Radiation properties of multi-band planar antennas with slits," *IEICE Trans. (B)*, vol. J89-B, no. 9, pp. 1589-1602, Sept. 2006.

[4] Y. Shinohe, M. Haneishi, and Y. Kimura, "Radiation properties of circularly-polarized multi-band planar antennas," *IEICE Trans. (C)*, vol. J89-C, no. 12, pp. 1019-1031, Dec. 2006.

[5] E. Nishiyama, K. Takanaka, and M. Aikawa, "Polarization controlled microstrip antenna," *IEICE Trans. (B)*, vol. J85-B, no. 9, pp. 1519-1525, Sept. 2002.

[6] Y.J. Sung, T.U. Jang, and Y.-S. Kim, "A reconfigurable microstrip antenna for switchable polarization," *IEEE Microw. Wireless Comp. Lett.*, vol. 14, no. 11, pp.534-536, Nov. 2004.

[7] F. Yang and Y. Rahmat-Samii, "Patch antennas with switchable slots (PASS) in wireless communications: concepts, designs, and applications," *IEEE Antennas Propagat. Mag.*, vol.47, no. 2, pp. 13-29, Apr. 2005.
[8] J.-S. Row and J.-F. Wu, "Aperture-coupled microstrip antennas with switchable polarization," *IEEE Trans. Antennas and Propagat.*, vol.54, no.9, pp.2686-2691, Sept. 2006.

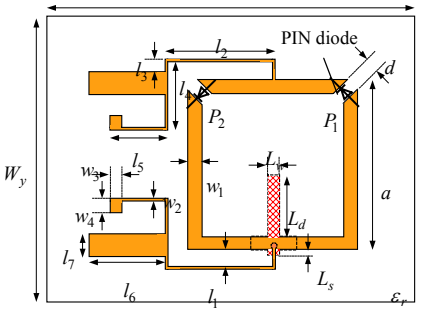

(a) Antenna element

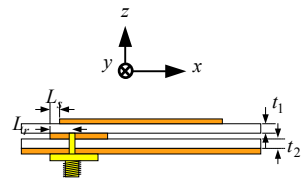

(b) Cross-sectional view

$$\left(\begin{array}{l} W_x = 70.0, W_y = 60.0, a = 21.5, w_1 = 1.6, w_2 = 0.4, w_3 = 3.0, w_4 = 3.4, \\ l_1 = 2.8, l_2 = 14.15, l_3 = 0.45, l_4 = 11.5, l_5 = 13.75, l_6 = 20.0, l_7 = 4.0, \\ d = 1.6, L_d = 10.0, L_w = 1.5, L_s = L_r = 0.5, t_1 = t_2 = 1.2, \text{unit : [mm]}, \quad \varepsilon_r = 2.6 \end{array}\right)$$

Figure 1: Configuration of a ring MSA with a bias circuit on the same layer.

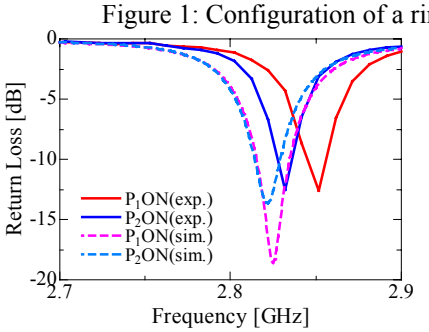

Figure 2: Return loss.

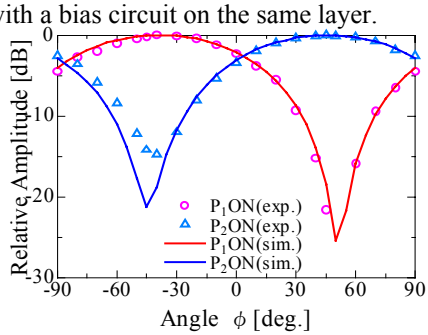

Figure 3: Polarization characteristics.

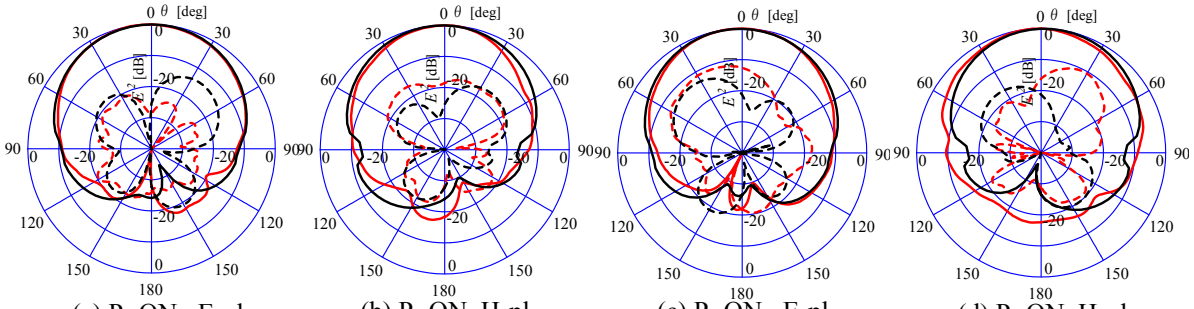

(a) P_1 ON , E-pl (b) P_2 ON, H-pl (c) P_1 ON , E-pl (d) P_2 ON, H-pl

—Sim. Co-pl. ···Sim. X-pl. , —Exp. Co-pl. ···Exp. X-pl.

Figure 4: Radiation pattern.

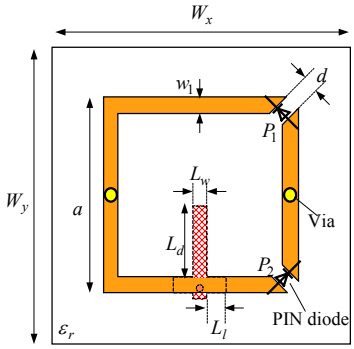

(a) Antenna element

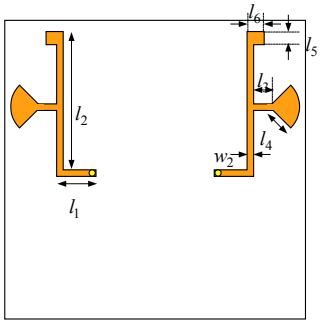

(a) Bottom view

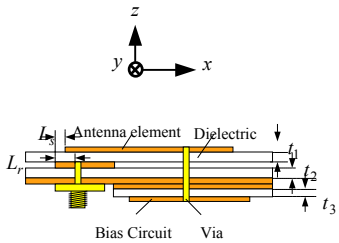

(c) Cross-sectional view

$$\left(\begin{array}{l} W_x = 60.0, W_y = 60.0, a = 21.5, w_1 = 1.6, w_2 = 0.5, l_1 = 8.0, l_2 = 21.25, l_3 = 5.0, l_4 = 6.0, l_5 = 3.0, l_6 = 3.5, \\ d = 1.6, L_d = 10.0, L_l = 7.0, L_w = 1.5, L_s = L_r = 0.5, t_1 = t_2 = 1.2, t_3 = 0.6, \text{ unit : [mm]}, \quad \varepsilon_r = 2.6 \end{array}\right)$$

Figure 5: Configuration of a ring MSA with a bias circuit on the backside of the ground plane.

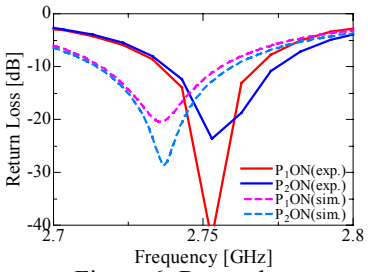

Figure 6: Return loss.

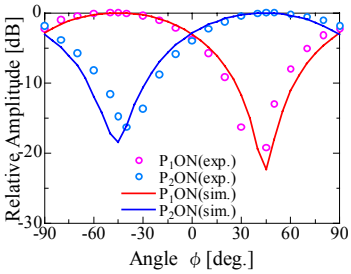

Figure 7: Polarization characteristics.

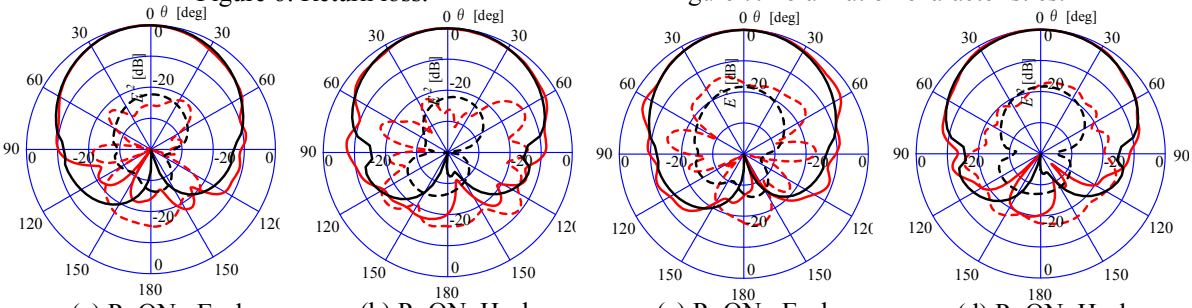

(a) P_1 ON , E-pl (b) P_2 ON, H-pl (c) P_1 ON , E-pl (d) P_2 ON, H-pl

—Sim. Co-pl. ···Sim. X-pl. , —Exp. Co-pl. ···Exp. X-pl.

Figure 8: Radiation pattern.

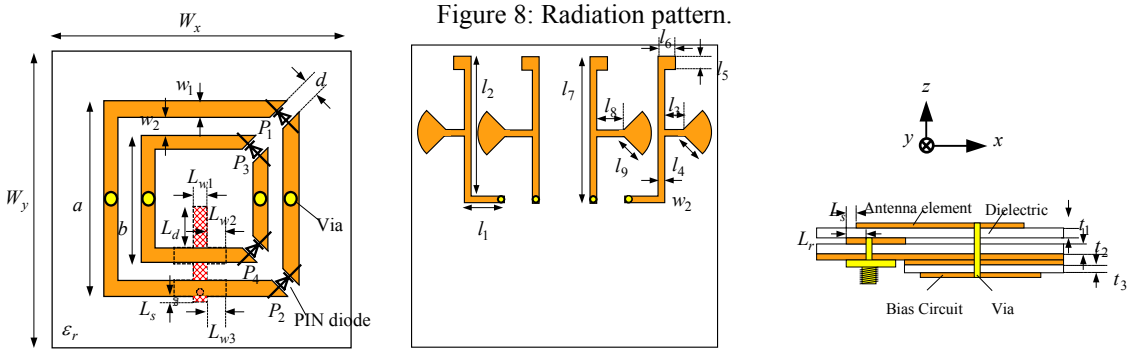

(a) Antenna element (a) Bottom view (c) Cross-sectional view

$$W_x = W_y = 60,, a = 21.5, b = 13.0, w_1 = 1.6, w_2 = 2.65, d = 1.6, L_d = 6.5, L_{w1} = 1.5, L_{w2} = 7.0, L_{w3} = 2.75, P_s = P_d = 0.5,$$
$$l_1 = 8.0, l_2 = 21.25, l_3 = 5.0, l_4 = 6.0, l_5 = 3.0, l_6 = 3.5, l_7 = 21.0, l_8 = 4.0, l_9 = 3.0, t_1 = t_2 = 1.2, t_3 = 0.6, \text{unit}: [\text{mm}], \quad \varepsilon_r = 2.6$$

Figure 9: Configuration of two ring MSAs with PIN diodes for dual band operation.

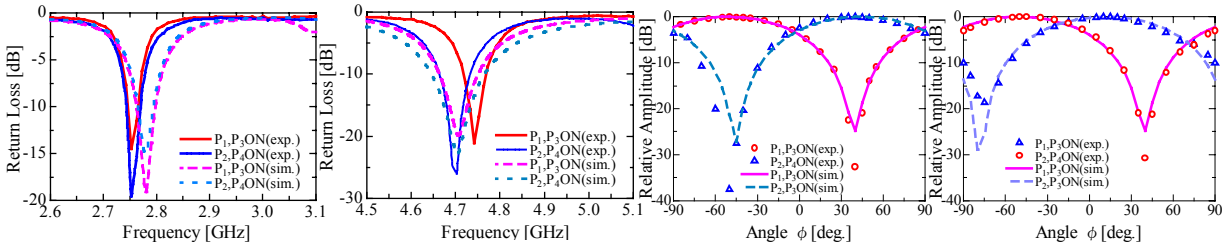

(a) 1st mode (b) 2nd mode

Figure 10: Return loss.

(a) 1st mode (b) 2nd mode

Figure 11: Polarization characteristics.

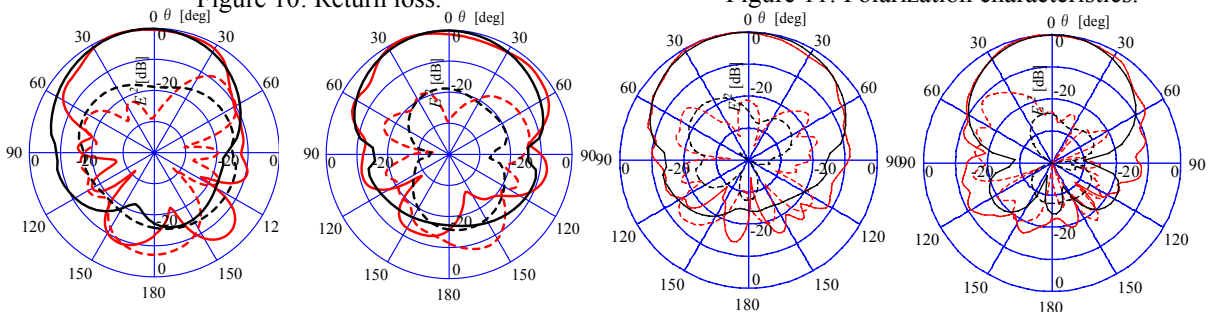

(a) 1st mode P_1 ,P_3ON, E-pl (b) 1st mode P_1 ,P_3ON, H-pl (c) 2nd mode P_1 ,P_3ON, E-pl (d) 2nd mode P_1 ,P_3ON, H-pl

—Sim. Co-pl. ···Sim. X-pl. , —Exp. Co-pl. ···Exp. X-pl.

Figure 12: Radiation Pattern.